Carbohydrate Polymer Technologies and Applications 14 (2026) 101128

Contents lists available at ScienceDirect

Carbohydrate Polymer Technologies and Applications

journal homepage: www.sciencedirect.com/journal/carbohydrate-polymer-technologies-and-applications

Tailoring the properties of rhamnose-rich exopolysaccharides from cheese whey *via* continuous fed-batch fermentation for active packaging applications

Samia Azabou [a], Ichrak Joulak [a], Patrícia Concórdio-Reis [b,c], Cristiana AV Torres [b,c], Chantal Sevrin [d], Christian Grandfils [d], Hamadi Attia [a], Adem Gharsallaoui [e,*], Filomena Freitas [b,c]

[a] Ecole Nationale d'ingénieurs de Sfax - Laboratoire Analyse, Valorisation et Sécurité des Aliments – Université de Sfax, Sfax, 3038, Tunisia
[b] Associate Laboratory i4HB - Institute for Health and Bioeconomy, NOVA School of Science and Technology, NOVA University Lisbon, Caparica, Portugal
[c] UCIBIO – Applied Molecular Biosciences Unit, Department of Chemistry, NOVA School of Science and Technology, NOVA University Lisbon, Caparica, Portugal
[d] Interfaculty Research Centre of Biomaterials (CEIB), University of Liège, Liège, Belgium
[e] Univ Lyon, Université Claude Bernard Lyon 1, CNRS, LAGEPP UMR 5007, F-69100 Villeurbanne, France

ARTICLE INFO

Keywords:
Halomonas caseinilytica K1
Exopolysaccharide
Fed-batch fermentation
Cheese whey valorization
Polysaccharide characterization
Antimicrobial films
Active packaging

ABSTRACT

This study explores the sustainable bioconversion of cheese whey (CW) into high-value exopolysaccharides (EPS) by *Halomonas caseinilytica* K1 through the optimization of bioreactor operation modes. Batch, fed-batch with pulse feeding, and fed-batch with continuous feeding were compared to evaluate their impact on cell growth, EPS production, and polymer characteristics. The continuous fed-batch strategy markedly outperformed the other modes, achieving the highest biomass concentration (89.95 g/L) and EPS titer (11.67 g/L), corresponding to 2.12- and 5.16-fold increases relative to pulse-fed and batch cultures, respectively. This cultivation approach significantly influenced EPS structure, yielding a rhamnose-enriched polymer with a high molecular weight of 2.25×10^5 Da, corresponding to a fourfold increase. The optimized EPS (EPS-K1-B3) was subsequently applied to fabricate biodegradable antimicrobial films incorporating geraniol (10%). These films displayed good structural integrity and demonstrated sustained inhibitory activity against *Escherichia coli* and *Listeria innocua* over a 22-day release period. Overall, this work establishes an integrated bioprocess–structure–function framework, demonstrating how controlled fermentation conditions can tailor EPS properties for targeted applications in active food packaging while contributing to the valorization of agro-industrial waste streams.

1. Introduction

The global transition toward sustainable and environmentally friendly packaging has intensified in recent years, driven by the need to mitigate the well-known limitations of fossil-based plastics. These conventional synthetic packaging materials, which are non-renewable and nonbiodegradable, present many drawbacks including the difficulty of disposal and recycling, leading to considerable environmental impacts. In addition, these materials rely on finite and insecure resources such as oil and petroleum, further raising concerns regarding their long-term sustainability (e.g. oil and petroleum) (Hassannia-Kolaee et al., 2016). In this context, numerous polysaccharides, such as cellulose, pectin, starch, chitosan, alginate, and carrageenan, have been widely explored for their film-forming ability (Cazon et al., 2017; Shiryanpour et al., 2025). However, their application is often limited by drawbacks such as high hydrophilicity resulting in poor moisture barrier properties and limited mechanical stability under humid conditions. In contrast, microbial exopolysaccharides (EPS) have likewise gained increasing attention as natural biopolymers due to their biodegradability, biocompatibility, non-toxicity and relatively straightforward extraction and purification procedures. In addition, their structure and composition can be modulated through microbial metabolism and fermentation parameters, enabling the production of polymers with tailored molecular weight, monosaccharide composition, and functional properties suitable for specific applications (Freitas et al., 2011). Despite this potential, their large-scale application in packaging remains constrained

* Corresponding author.
E-mail address: adem.gharsallaoui@univ-lyon1.fr (A. Gharsallaoui).

https://doi.org/10.1016/j.carpta.2026.101128

Available online 25 March 2026

by typically low production yields and high manufacturing costs, largely associated with substrate requirements and downstream processing (Freitas et al., 2011). For instance, although levan, dextran and xanthan exhibit promising functional properties, their application in packaging is still restricted by the need of refined sugars for fermentation and the high recovery cost (Freitas et al., 2011; Garcia-Ochoa et al., 2000; Öner et al., 2016). Thus, developing efficient cultivation strategies combining the use of low-cost substrates such as low-cost agro-industrial by-products with optimized fermentation strategies is essential to improve process economics and make microbial EPS competitive with polysaccharides from other sources.

Cheese whey (CW), the liquid byproduct of cheese manufacture, is produced in very large volumes globally due to the scale of the dairy industry. The world production of CW is estimated to exceed 190 million tons/year. According to the latest Eurostat data on milk and dairy products (https://ec.europa.eu/), the dairy industry in the European Union generates around 15 million tons of CW annually, whereas, the Tunisian CW production is estimated at approximately 35.000 tons/year (Mabrouki et al., 2022). CW contains substantial levels of fermentable carbohydrates and soluble proteins, rendering it increasingly interesting for conversion into value-added microbial metabolites such as EPS through its use as a substrate in biotechnological processes (Antunes et al., 2015). Besides reducing production costs, the use of CW as a feedstock contributes to establishing sustainable waste valorization pathways by transforming this by-product into functional EPS, thus creating a direct bridge between circular resource utilization and the development of bio-based materials like active packaging applications.

Efficient cultivation strategies can also markedly improve EPS yields, as bioreactors allow tight control and standardization of environmental conditions. Under such controlled settings, both productivity optimization and targeted modulation of EPS physicochemical properties become more accessible (Seviour et al., 2011). Batch cultivation is widely employed to identify suitable conditions for microbial growth and EPS synthesis (Radchenkova et al., 2014). However, this mode is inherently limited by substrate depletion or by the accumulation of inhibitory metabolites such as organic acids like pyruvate and higher concentration of dissolved CO_2, which may ultimately restrict biomass formation and EPS production (Gonzalez-Garcia et al., 2015). In contrast, fed-batch cultivation offers a more attractive alternative for producing higher amounts of EPS, by improving the overall bioprocess productivity and shortening the required fermentation time. This approach consists of an initial batch phase followed by a feeding stage, either through substrate pulses or continuous feeding, without removal of the culture broth (Liu et al., 2008). Fed-batch processes are particularly advantageous when product formation is coupled to microbial growth, as they sustain cell activity and prevent nutrient limitation (Yang & Sha, 2022).

In a previous study, the ability of four *Halomonas* strains to grow on different low-cost substrates (cheese whey, glycerol, grape pomace) was evaluated, and *H. caseinilytica* K1 emerged as the most efficient EPS producer on CW (Joulak et al., 2022). Building on these findings, the present work aims to scale up EPS production from shaking-flask cultures to stirred-tank bioreactors operated under distinct modes, batch, fed-batch with pulse feeding, and fed-batch with continuous feeding, using CW as a renewable carbon source. The impact of fermentation strategy on bacterial growth, EPS yield, and EPS structural features was assessed. Additionally, the potential of the recovered EPS to serve as a novel biomaterial for biodegradable antimicrobial films was examined.

Based on these considerations, we hypothesized that controlling carbon and nitrogen availability through fed-batch fermentation would modulate the molecular weight distribution and monosaccharide composition of the exopolysaccharide produced by *Halomonas caseinilytica* K1, thereby enhancing its film-forming ability and antimicrobial functionality for active packaging applications. To the best of our knowledge, this is the first study that investigates EPS production by *H. caseinilytica* K1 under multiple bioreactor configurations and demonstrates its applicability as a film-forming material.

2. Materials and methods

2.1. Microorganism and media

The bacterial strain *H. caseinilytica* K1 (JCM 32859) used in all experiments was previously isolated from the solar saltern of Kerkennah, in Tunisia (Joulak et al., 2019). The semi-complex medium (SCM) composed of (g/L): NaCl, 50; $MgCl_2{\cdot}6H_2O$, 13; $MgSO_4{\cdot}7H_2O$, 9; KCl, 1.3; $CaCl_2{\cdot}2H_2O$, 0.2; NaBr, 0.15; $NaHCO_3$, 0.05; yeast extract, 0.3 and peptone 0.2 (Joulak et al., 2019), was used to reactivate the culture from a cryo-preserved stock and for inocula preparation. For the bioreactor experiments, SCM was supplemented with a sterile concentrated CW aqueous solution (40%, w/v) (supplied by Lactogal Produtos Alimentares S.A. Portugal) to reach around 4% (w/v) of initial lactose concentration. CW had a lactose content of 78.40 wt.%, as well as 13.62 wt.% protein, 1.21 wt.% fat and 0.89 wt.% lactic acid (Joulak et al., 2022).

2.2. Bioreactor cultivation

Cell growth and EPS production studies were conducted in 2 L stirred-tank bioreactors (BioStat B, Sartorius, Germany). Inocula for the bioreactor experiments were prepared by incubating culture flasks at 30 °C containing SCM supplemented with 1% (w/v) of glucose, during 24 h in an orbital incubator (150 rpm). Each assay was started once the bioreactor (containing 1.8 L of SCM supplemented with CW) was inoculated (10% (v/v)). Temperature (30±0.1 °C), pH (7.0 ± 0.05), and aeration rate (0.4 standard liters per min (SLPM)) were maintained constant during each cultivation as follows. For the batch bioreactor operated for 72 h, dissolved oxygen concentration (dO_2, % saturation) was controlled at 10% of the air saturation by automatic variation of the stirrer speed (300–800 rpm) and pH was adjusted to 7.0 through the automatic addition of HCl (5 M) or NaOH (5 M). The fed-batch bioreactor (pulsed and continuous feeding of CW) was investigated for 48 h with an initial batch phase starting from a lactose concentration of 4% (w/v). During the fed-batch phase, the dO_2 was controlled at 20% by the automatic variation of the substrate-feeding rate. pH was adjusted to 7.0 with HCl (5 M) or ammonium (0.25%, v/v) instead of NaOH. The pulse or continuous feeding was started when the dO_2 in the bioreactor increased above 20%. For the pulse-fed experiment, 100 mL of concentrated solution of CW (40%, w/v) were provided at 22 and 32 h. For the continuously fed experiment, the feeding was initiated at 6 h using an initial lactose feeding rate of 5 mL/h, which was incremented to 7.5, 15, 20, 22.5, and 25 mL/h at 8, 22, 26, 29, and 33 h, respectively. During fermentations, aliquots were aseptically taken for biomass, EPS, sugars, and ammonium quantification.

2.3. Analytical techniques

The cell dry weight (CDW) was determined using a gravimetric method. Culture broths were centrifuged at 15,652 × *g*, for 20 min, at 4 °C. Then, the bacterial cell pellets were washed twice with deionized water, centrifuged as described above and freeze-dried. Quantification of sugars (lactose, glucose and galactose) in the supernatant samples was performed using high performance liquid chromatography (HPLC), equipped with a MetaCarb 87H column (Varian) with refractive index detection, using lactose, glucose and galactose as internal standards (Antunes et al., 2015). Ammonium concentration was quantified by segmented flow analysis (Skalar 5100, Skalar Analytical, The Netherlands) using ammonium chloride as standard. Protein concentration in the supernatant was estimated by the method of Bradford (1976). For EPS gravimetric quantification, the cell-free supernatant was dialyzed using a 10 kDa MWCO membrane (SnakeSkinTM Pleated Dialysis Tubing, Thermo Scientific) against deionized water, as extensively detailed by Joulak et al. (2022). Finally, the purified EPS was freeze-dried and weighed.

2.4. Kinetics parameters

The determination of the maximum specific growth rate (μ_{max}, 1/h), the yields of biomass ($Y_{X/S}$, $g_{CDW}/g_{Total\ sugars}$) and EPS ($Y_{P/S}$, $g_{EPS}/g_{Total\ sugars}$) on a substrate basis and the EPS volumetric productivity (r_P, g_{EPS}/(L.h)) was previously deeply described by Joulak et al. (2022).

2.5. EPS extraction

After each cultivation run, the culture broth recovered from the bioreactor was centrifugated (15,652 × g, 20 min, 4 °C) to finally discard cell pellets. The resultant cell-free supernatant was treated at 70 °C during 1 h, followed by a centrifugation (15,652 × g, 1 h, 4 °C) to remove any remaining cell debris and denatured proteins (Concordio-Reis et al., 2021) and dialysis using as described above. Finally, the solution was lyophilized, and the obtained polymer was stored at room temperature in closed vessels.

The successive steps of thermal treatment, centrifugation, dialysis, and lyophilization ensured the removal of residual cells, proteins, and low-molecular-weight compounds, yielding purified EPS suitable for subsequent structural characterization and film-forming applications.

2.6. EPS characterization

2.6.1. Monosaccharide composition

EPS samples (5 mg) were subjected to hydrolysis with trifluoroacetic acid (0.1 mL), at 120 °C, for 2 h. Identification and quantification of the constituent monosaccharides present in the obtained hydrolysates were performed using HPLC equipped with a CarboPac PA10 column (Thermo Scientific™ Dionex™, Sunnyvale, CA, USA), and an amperometric detector (Concordio-Reis et al., 2021). Glucose, galactose, glucuronic acid, rhamnose, ribose and arabinose (Sigma-Aldrich) were used as standards (1–100 ppm). A Carbopac SA10 4 × 250 mm column (Thermo Scientific™ Dionex™, Sunnyvale, CA, USA) and the same amperometric detector were used for mannose identification and quantification.

2.6.2. Molecular mass distribution

Molecular weight (M_w) was obtained by the size exclusion chromatography coupled with multi-angle light scattering (SEC-MALS), according to Concordio-Reis et al. (2021).

2.7. Film-forming properties

2.7.1. Preparation of antimicrobial EPS/geraniol-based films

Film forming of oil/water emulsion was prepared with 2% EPS, 0.8% glycerol as plasticizer, and 10% geraniol as antimicrobial agent. The solutions (2%, w/w) were obtained by dissolving the lyophilized EPS in imidazole/acetate buffer (5 mM), at pH 5.0, and stirring overnight at room temperature. Afterwards, glycerol and geraniol were mixed to the EPS solution, using an Ultra Turrax T-18 basic (IKA, Germany), for 10 min at 20 000 rpm. Films were prepared by transferring 20 g of film-forming solution to glass Petri dishes (65 mm diameter × 15 mm height) and drying at 40 °C for 3 days. Dry films were then peeled intact from the casting surface. EPS-based films (2% (w/w) EPS and 0.8% (w/w) glycerol) were also prepared in the same conditions and used as control films (Joulak et al., 2023).

2.7.2. Film thickness and color measurement

The film thickness was measured with a hand-held micrometer (Mitutoyo IP65 Digimatic Coolant-Proof Micrometer). Three random locations around each film sample were used for thickness determination. Color properties of films were evaluated using the CIELAB color notation system (International Commission on Illumination) that expresses color as three values: lightness L* (lightness), a* (red-green) and b* (yellow-blue). These values are given by a colorimeter (Chroma meter CR-5, Konica Minolta, INC, Japan), calibrated with black and white tiles.

2.7.3. Antimicrobial activity

Stock cultures of *Escherichia coli* (DSM 682) and *Listeria innocua* (ATCC 33,090) were used to prepare sub-cultures and then pre-cultures in tryptone soy broth (TSB, Biokar Diagnistics, France) at 10% (v/v). This pre-culture (1 mL) was transferred into 9 mL of TSB and incubated at 37 °C, for 5 h. Afterwards, the bacterial cells were diluted in tryptone salt broth to reach a concentration of 1×10^6 CFU/mL, and incorporated in tryptone soy agar (TSA) at 5% (v/v). The EPS-based films, plain (control) and those containing geraniol-in-water emulsion, were cut into discs (9 mm in diameter), which were placed on the TSA plates inoculated with *E. coli* or L.*innocua.* The plates were first incubated at 4 °C, for 2 h, and then at 37 °C, for 24 h. The antimicrobial activity was evaluated by measuring the inhibition zone diameters (IZD), after 24 h of incubation (Joulak et al., 2023). Then, the kinetics of the antimicrobial activity of EPS-based films were assessed throughout 30 days at 37 °C, *via* the determination of IZD around EPS-based films according to Joulak et al. (2023).

2.8. Statistical analysis

All analytical determinations were performed in duplicate and results were expressed as means ± standard deviations. One-way analysis of variance (ANOVA) with Tukey's test was conducted to determine any significant data differences between the groups of samples. Difference was considered statistically significant when p-value$<$ 0.05 using the software IBM SPSS V. 21.

3. Results and discussion

3.1. Enhancing EPS production via fermentation process

3.1.1. Batch cultivation

The batch cultivation strategy was first implemented to monitor both cell growth and EPS synthesis by *H. caseinilytica* K1. The culture medium consisted of SCM supplemented with a concentrated CW solution (40%, w/v), providing an initial lactose concentration of approximately 40 g/L. According to the CW composition, the medium also contained about 6.81 wt.% protein, 0.61 wt.% fat, and 0.45 wt.% lactic acid. As shown in Fig. 1a, EPS production occurred concomitantly with biomass accumulation, with a specific growth rate of 0.14 ± 0.05 h^{-1} (Table 1). The culture reached a maximum CDW of 3.06 ± 0.15 g/L after 48 h. During this period, lactose concentration decreased from 39.53 to 13.82 g/L, while glucose and galactose released from lactose hydrolysis were fully consumed within the first 9 h. Ammonium depletion occurred even earlier, being exhausted within 7 h of cultivation. Under these nitrogen-limiting conditions, strain K1 likely relied on CW proteins as an alternative nitrogen source to sustain rapid cell growth and EPS synthesis (Fig. 1), consistent with the growth-associated nature of EPS production previously reported (Joulak et al., 2022).

In this batch process, the EPS concentration reached 2.26 ± 0.30 g/L (Table 1), a value substantially higher than that obtained in shaken-flask cultures (0.446 ± 0.014 g/L; Joulak et al., 2022). Likewise, the volumetric EPS productivity (1.23 ± 0.25 g EPS/(L·h)) markedly exceeded the productivity at shake-flask scale (0.112 ± 0.06 g EPS/(L·h)). Overall, batch cultivation resulted in a fivefold increase in EPS concentration and a tenfold improvement in productivity compared with flask cultures. This could be due to enhanced process control when fermentation is performed in small bioreactors, equipped with pH, temperature and dissolved oxygen concentration probes, promoting thus higher biomass and EPS concentration, whereas flasks are limited by low oxygen transfer and lack of monitoring (Freitas et al., 2011).

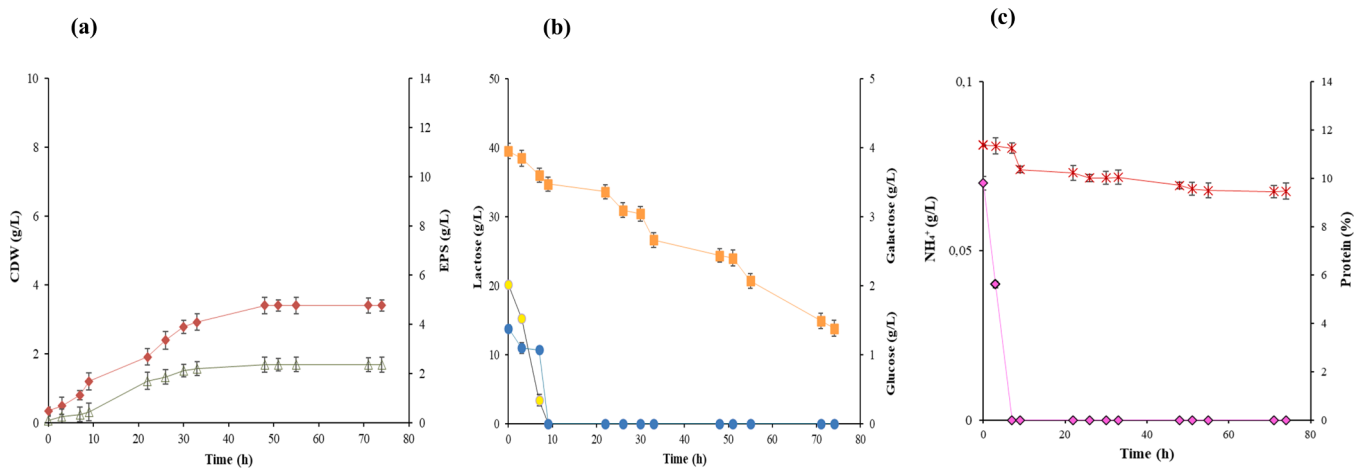

Fig. 1. Cultivation profile obtained in batch culture of Halomonas caseinilytica K1, using cheese whey as substrate: (a) CDW (◆) and EPS (Δ) ; (b) lactose (■), glucose (●) and galactose (●); (c) ammonium (◆) and protein (×).

Table 1
Kinetic and stoichiometric parameters obtained in the bioreactor cultivation of H. caseinilytica K1 using different cultivation strategies.

Cultivation strategy	CDW (g/L)	μmax (h-1)	EPS (g/L)	rP (gEPS/L.h)	ΔS (g/L)	YP/S (gEPS/gS)	Reference
Shake flask	4.81±0.42[a]	ND	0.446±0.014[a]	0.112±0.06[a]	16.02±1.50[a, (1)]	ND	Joulak et al. (2022)
Batch	3.06±0.15[a]	0.14±0.05[a]	2.26±0.30[b]	1.23±0.25[b]	29.10±1.25[b, (3)]	0.08±0.04[a, (4)]	This study
Fed-batch with pulse feeding	8.13±0.30[b]	0.24±0.06[a,b]	5.49±0.35[c]	2.75±0.28[c]	37.00±0.85[c, (3)]	0.15±0.06[a, b (4)]	This study
Fed-batch with continuous feeding	89.95±3.18[c]	0.39±0.06[b]	11.67±0.70[d]	5.60±0.32[d]	46.93±1.02[d, (3)]	0.25±0.05[b, (4)]	This study

(1): lactose consumption; (2): on a lactose basis; (3): Total sugars consumption, (4) on a total sugars basis; ND: Not Determined.
*Values in the same column with different letters are significantly different at $p < 0.05$.

3.1.2. Fed-batch cultivation

3.1.2.1. Fed-batch cultivation with pulse feeding. The first fed-batch fermentation consisted of an initial batch phase conducted under the same conditions as described above, except that pH regulation was ensured by the automatic addition of NH_4OH instead of NaOH. Besides its buffering role, NH_4OH provided an additional nitrogen source, thereby increasing nitrogen availability for cell growth. After approximately 22 h of cultivation, the dissolved oxygen (dO_2) began to rise above the 20% setpoint, indicating carbon source depletion. At this point, a 100 mL pulse of concentrated CW solution (40%, w/v) was added (Fig. 2). A second rise in dO_2 was observed at 32 h, triggering a second pulse addition.

As shown in Fig. 2, *H. caseinilytica* K1 maintained exponential growth during the entire fed-batch phase, with no detectable lag period, while sugars were continuously consumed. The biomass concentration reached 8.13 ± 0.30 g/L at 48 h, corresponding to a 2.65-fold increase compared with batch cultivation (3.06 ± 0.15 g/L). This confirms the strong positive impact of the pulse-fed strategy on cell growth, consistent with previous reports highlighting the suitability of fed-batch modes for efficient biomass accumulation and precise fermentation control (Han et al., 2018).

During the fed-batch phase, glucose and galactose were almost completely consumed, whereas lactose concentrations after each pulse remained above 24.38 g/L, the minimal value reached in batch cultures before growth cessation. In the final stage of cultivation (32–48 h),

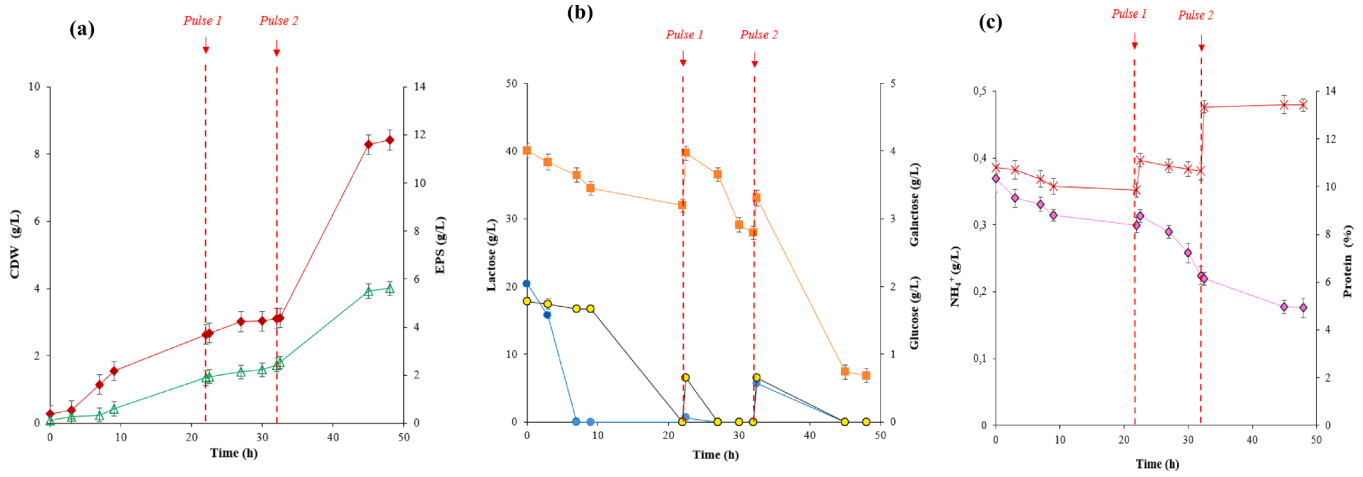

Fig. 2. Cultivation profile obtained in fed-batch culture of Halomonas caseinilytica K1, under pulse substrate feeding, using cheese whey as substrate : (a) CDW (◆) and EPS (Δ) ; (b) lactose (■), glucose (●) and galactose (●) ; (c) ammonium (◆) and protein (×).

lactose levels dropped markedly; however, both biomass and EPS production plateaued despite the continuous availability of nitrogen.

As shown in Table 1, the maximum specific growth rate increased to 0.24 ± 0.06 h^{-1}, likely due to improved nitrogen supply resulting from NH_4OH addition. EPS production was also enhanced: EPS concentration (5.49 ± 0.35 g/L) and volumetric productivity (2.75 ± 0.28 g EPS/(L·h)) increased by factors of 2.42 and 2.24, respectively, compared with batch fermentation (2.26 ± 0.30 g/L and 1.23 ± 0.25 g EPS/(L·h)). The product yield YP/S reached 0.15 ± 0.06 g EPS/g total sugars. This improvement can be attributed to the sustained and synchronized availability of carbon and nitrogen sources, enabling continuous cell growth and subsequent EPS biosynthesis, which accumulated in the medium.

3.1.2.2. Fed-batch cultivation with continuous feeding. The fed-batch experiment with continuous CW feeding was performed after an initial 48 h batch phase, using a feeding profile progressively increasing from 5 to 25 mL/h. This strategy resulted in a remarkable improvement in biomass formation: the culture reached 89.95 ± 3.18 g/L (Fig. 3), which represents an 11-fold increase compared with the pulse-fed mode (8.13 ± 0.30 g/L) and a 26.45-fold increase relative to batch cultivation (3.06 ± 0.15 g/L). Despite continuous substrate addition, all sugars were depleted after only 22 h of cultivation (Fig. 3b), indicating extremely rapid carbon uptake by *H. caseinilytica* K1.

The maximum specific growth rate further increased, reaching 0.39 ± 0.06 h^{-1} (Table 1). This enhanced growth performance likely reflects the sustained availability of ammonium and CW-derived proteins, which together supported a more favorable nitrogen balance for biosynthesis. Under these optimized conditions, the continuous feeding mode yielded the highest EPS production metrics among all tested strategies. The product yield (YP/S) and volumetric productivity reached 0.25 ± 0.05 g EPS/g total sugars and 5.60 ± 0.32 g EPS/(L·h), respectively. The final EPS concentration was 2.12 times higher than in the pulse-fed culture and 5.16 times higher than in batch mode (Table 1).

Overall, these results demonstrate that increasing carbon and nitrogen availability throughout the fermentation markedly enhances EPS synthesis by *H. caseinilytica* K1.

Maintaining continuous nutrient supply likely favors the formation of sugar nucleotide precursors required for EPS biosynthesis. As suggested by Sutherland (2011), extended growth periods support the accumulation of isoprenoid lipid carriers in the bacterial cell membrane, which are essential for EPS polymerization and secretion. This mechanistic rationale aligns with the substantial increase in EPS production observed under continuous feeding conditions. Additionally, the dO_2 concentration played a crucial role in regulating the balance between biomass formation and EPS synthesis. Maintaining the dO_2 at 20% air saturation ensured the culture remained under fully aerobic conditions throughout the fed-batch phase, preventing oxygen limitation (Garcia-Ochoa et al. 2010). Adequate oxygen availability supports efficient oxidative phosphorylation and ATP generation, which are essential for both cellular growth and the formation of activated sugar nucleotides involved in EPS biosynthesis (Lv et al., 2020). At the same time, maintaining such a dO_2 may have favored a balanced metabolic state wherein excess carbon could be redirected toward EPS synthesis rather than being completely channeled into cell growth (Radchenkova et al., 2014). This controlled oxygen regime likely contributed to sustaining both the high specific cell growth rate and the enhanced EPS productivity observed under continuous feeding conditions.

3.2. EPS characterization

The EPS samples recovered from *H. caseinilytica* K1 cultures grown under the different bioreactor configurations were analyzed in terms of monosaccharide composition and molecular weight distribution. This analysis aimed to determine how the cultivation strategy influenced the structural properties of the resulting biopolymers.

3.2.1. Monosaccharide composition

Each EPS sample obtained from the three bioreactor configurations, EPS-K1-B1 (batch culture), EPS-K1-B2 (fed-batch with pulse feeding), and EPS-K1-B3 (fed-batch with continuous feeding), was analyzed for monosaccharide composition and molecular weight distribution (Table 2). All samples exhibited broadly similar qualitative profiles, with galactose and rhamnose as the dominant constituents, and smaller amounts of glucose, mannose, ribose, arabinose, and glucuronic acid.

However, notable differences in the molar ratios of these monosaccharides were observed. For example, EPS-K1-B1 contained higher proportions of galactose (35 mol%) and rhamnose (30 mol%) compared with the EPS produced in shake-flask cultures (29 mol% and 26 mol%, respectively). In contrast, EPS-K1-B2 and EPS-K1-B3 were enriched in rhamnose (36 mol% and 32 mol%, respectively) and exhibited lower galactose contents (26 mol% and 24 mol%, respectively). Such variations are consistent with previously reported EPS from halophilic bacteria, in which rhamnose is frequently present but in differing proportions, as seen for *Vibrio* sp. QY101 (Jiang et al., 2011) and *Alteromonas macleodii* (Le Costaouëc et al., 2021). Rhamnose-rich EPS are increasingly valued due to their physicochemical and bioactive properties, offering potential applications in the food, cosmetic, and

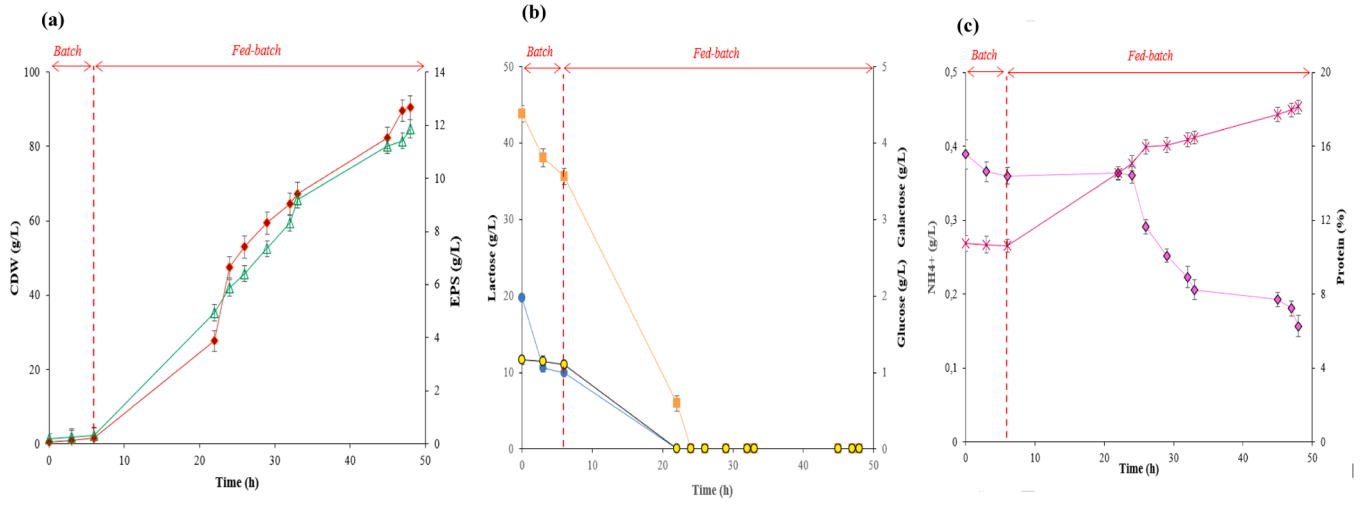

Fig. 3. Cultivation profile obtained in fed-batch culture of Halomonas caseinilytica K1, under continuous substrate feeding, using cheese whey as substrate : (a) CDW (◆) and EPS (Δ) ; (b) lactose (■), glucose (●) and galactose (●) ; (c) ammonium (◆) and protein (×).

Table 2
Monosaccharide composition and molecular weights (Mw) and polydispersity index (PDI) of EPS (K1-SF, K1-B1, K1-B2 and K1-B3).

	Monosaccharides (mol%)							Mw (kDa)	PDI	References
	Gal	Rha	Glu	Man	Rib	Ara	GlcA			
EPS-K1-SF	29	26	14	13	7	6	5	5.45×10^4	1.17	Joulak et al. (2022)
EPS-K1-B1	35	30	13	7	6	5	4	5.41×10^4	1.41	This study
EPS-K1-B2	26	36	15	9	6	5	3	6.05×10^4	1.47	This study
EPS-K1-B3	24	32	17	11	8	5	3	2.25×10^5	2.10	This study

K1-SF: from shake flask culture; EPS K1-B1: from batch culture; EPS K1-B2: from pulse feeding and EPS K1-B3: from continuous feeding.

biomedical sectors. These include their use as precursors for flavor/aroma formation and their relevance in anti-aging formulations (Robert et al., 2012).

Overall, the results indicate that the cultivation mode significantly affects the monosaccharide composition of EPS. This aligns with previous studies showing that EPS variability can arise from factors such as nutrient accessibility, fermentation conditions, precursor availability, and the activity of enzymes involved in sugar nucleotide biosynthesis (Malick et al., 2017).

In addition to neutral sugars, all EPS samples contained measurable amounts of glucuronic acid (Table 2), confirming the anionic nature of the polymers. The presence of uronic acid residues introduces negatively charged carboxylate groups along the polysaccharide backbone, which are known to influence intermolecular interactions, hydration behavior, and macromolecular organization in aqueous systems. Such anionic character is frequently reported for EPS produced by halophilic bacteria and plays a key role in their physicochemical and functional properties.

3.2.2. *Molecular mass distribution*

As shown in Table 2, the molecular weights of EPS-K1-SF, EPS-K1-B1, and EPS-K1-B2, obtained respectively from shake-flask, batch, and pulse-fed cultures, were relatively similar, with Mw values of 5.45×10^4, 5.41×10^4, and 6.05×10^4 Da. In contrast, a marked increase in molecular weight was observed for EPS-K1-B3 recovered from the continuous feeding strategy, which displayed an Mw of 2.25×10^5 Da. This nearly fourfold increase highlights the strong influence of the continuous-fed bioprocess on polymer biosynthesis, suggesting that the sustained nutrient availability favored the production of higher-molecular-weight EPS.

Beyond the increase in average molecular weight, the EPS produced under continuous fed-batch conditions (EPS-K1-B3) also exhibited a higher dispersity (PDI), indicating a broader molecular weight distribution. The combination of high Mw and increased PDI is known to promote chain entanglement and intermolecular associations, which are critical factors for the formation of cohesive and mechanically stable polysaccharide networks. In the present study, these structural features are consistent with the enhanced film-forming ability observed for EPS-K1-B3, supporting its suitability as a matrix for antimicrobial film development.

The high Mw observed for the EPS produced in the continuous fed-batch assay is likely due to the sustained substrate availability during cultivation that likely provided more balanced metabolic conditions. Continuous feeding allows for a steadier supply of carbon and nitrogen, ensuring that glycosyltransferases have a constant pool of activated sugar nucleotides to elongate the polymer chains. Unlike batch or pulse-fed systems, where rapid substrate depletion or metabolic stress can terminate chain elongation prematurely, the fed-batch continuous mode maintains moderate growth rates and sufficient energy and cofactor levels, enabling prolonged polymerization (Liu et al., 2025). This stable environment may allow a more efficient functioning of the biosynthetic machinery, producing EPS of significantly higher molecular weight compared with other feeding strategies.

3.3. *Application in active packaging*

Antimicrobial films incorporating natural bioactive molecules are increasingly considered promising tools to inhibit foodborne pathogens. In this study, the EPS obtained under continuous feeding (EPS-K1-B3), characterized by a high Mw and a high rhamnose content, was evaluated as a film-forming material for the incorporation of geraniol, an essential oil with broad antimicrobial activity and GRAS status (Petchwattana et al., 2021). In fact, the presence of deoxy sugars with moderate hydrophobicity confers rhamnose-rich EPS a partially amphiphilic character (Poli et al., 2010) rendering them particularly attractive for film formation as it promotes stronger intermolecular cohesion through combined hydrogen bonding and hydrophobic interactions, leading to dense, flexible, and mechanically stable films with improved moisture resistance (Freitas et al., 201). In contrast, more common EPS such as xanthan and levan are highly hydrophilic and often form brittle or weak matrices that are sensitive to humidity (Garcia-Ochoa et al., 2000; Öner et al., 2016). Moreover, the surface-active nature of rhamnose-rich EPS could enhance coating uniformity and facilitates the incorporation of antimicrobial agents such as geraniol ensuring a more homogenous distribution within the film matrix, and their controlled release, which is essential for active packaging applications (Freitas et al., 2011).

3.3.1. *Film appearance, thickness, and color properties*

The macroscopic appearance of the films is presented in Fig. 4. Both types of EPS-based films displayed a uniform yellow coloration and a visually homogeneous surface. No cracks, granules, or phase-separated domains were observed, indicating good compatibility between EPS, glycerol, and geraniol. The control EPS film (Fig. 4a) exhibited a smooth, translucent surface, whereas the EPS/geraniol film (Fig. 4b) showed a slightly rougher and more compact texture, which is consistent with the incorporation of a hydrophobic compound into a hydrophilic matrix.

Colorimetric parameters (Table 3) confirmed that the addition of geraniol significantly affected the visual properties of the films. The EPS/geraniol films displayed higher L*, a*, and b* values, corresponding to lighter, more reddish, and more yellowish tones. This change in

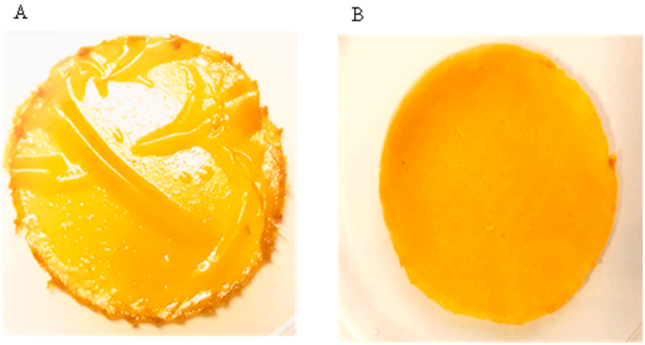

Fig. 4. Visual appearance of EPS-based film (A) and EPS/geraniol-based film (B).

Table 3
Color coordinates and thickness of EPS-based films.

	L^*	a^*	b^*	Thickness (mm)
EPS-film	$41.17^{a} \pm 0.15$	$3.99^{a} \pm 0.06$	$22.90^{a} \pm 0.17$	$0.018^{a} \pm 0.002$
EPS/geraniol-film	$52.61^{b} \pm 0.54$	$6.35^{b} \pm 0.16$	$28.52^{b} \pm 0.22$	$0.056^{b} \pm 0.004$

Values in the same column with different letters are significantly different at $p < 0.05$.

optical properties suggests that geraniol altered the internal light scattering behavior of the matrix, consistent with the microstructural differences visible in Fig. 4.

Although all films were cast using identical masses of film-forming solution, their thicknesses differed significantly. The control EPS film had a thickness of 0.018 ± 0.002 mm, while the EPS/geraniol film reached 0.056 ± 0.004 mm ($p < 0.05$). This increase is consistent with previous reports indicating that incorporation of low–molecular weight essential oils can disrupt polymer–polymer interactions and slightly expand the polymeric network (Haghighi et al., 2019). As shown in Fig. 4, the visual differences in morphology correspond well to the measured differences in thickness.

3.3.2. *Antimicrobial activity and release kinetics of EPS/geraniol films*

The antimicrobial activity of the films was evaluated by direct contact of the film discs with inoculated TSA plates. As expected, the control EPS film exhibited no inhibitory effect against *E.coli* or *Listeria innocua*. In contrast, the EPS/geraniol film produced a clear inhibition halo against both strains, confirming the successful diffusion of geraniol through the EPS matrix. The kinetics of antimicrobial activity over 30 days are shown in Fig. 5.

The inhibition zone diameter (IZD) increased progressively until day 22 for both microorganisms, reflecting a sustained and controlled release of geraniol from the film. Beyond this period, the antimicrobial activity tended to plateau, indicating stabilization of the release rate. Consistent with typical microbial susceptibilities, L.*innocua* displayed larger inhibition zones (up to 2.5 cm) than *E. coli* (2.1 cm). This difference is attributed to the structural characteristics of Gram-positive bacteria, which lack the outer membrane and associated lipopolysaccharides that hinder penetration of hydrophobic antimicrobials in Gram-negative bacteria (Ouattara et al., 1976).

The sustained antimicrobial activity observed over 22 days may be related to the molecular interactions occurring between geraniol and the EPS matrix. The anionic character of the EPS, resulting from the presence of glucuronic acid residues, provides carboxylate and hydroxyl groups capable of forming intermolecular interactions with geraniol molecules. In particular, hydrogen bonding may occur between the hydroxyl group of geraniol and the hydroxyl or carboxyl groups of the polysaccharide chains. In addition, the partial amphiphilic character of the rhamnose-rich EPS may promote hydrophobic associations with the non-polar moieties of geraniol. These combined interactions likely contribute to the temporary retention of geraniol within the polymer network, leading to its progressive diffusion and the sustained antimicrobial activity observed over time.

Together, these results demonstrate that EPS-K1-B3 constitutes a suitable matrix for the development of biodegradable antimicrobial films, with well-defined structural integrity and controlled release properties.

3.4. *Linking bioprocess conditions, EPS structural features, and film functionality*

The combined results obtained from the different cultivation strategies demonstrate a clear relationship between bioprocess conditions, the structural attributes of the EPS produced, and their resulting functional performance in active packaging applications. The continuous feeding strategy, which ensured sustained availability of carbon and nitrogen sources, yielded the highest biomass and EPS production levels. This optimized bioprocess not only improved productivity but also influenced the molecular characteristics of the polymer, particularly by generating EPS with a markedly higher molecular weight (2.25×10^5 Da) and a specific monosaccharide profile enriched in rhamnose. Such structural features directly contributed to the enhanced film-forming behavior observed for EPS-K1-B3. The polymer enabled the fabrication of homogeneous and mechanically coherent films capable of effectively incorporating geraniol and ensuring its gradual diffusion over time. The controlled and prolonged antimicrobial activity observed throughout 22 days highlights the advantage of the developed active materials in providing sustained protection against spoilage microorganisms, a performance characteristic largely absent in traditional petroleum-derived films without added bioactive agents (Petchwattana et al., 2021). In fact, most commercial packaging polymers (e.g., PLA and LDPE) lack intrinsic antimicrobial functionality and act mainly as passive barriers, while active films embedded with antimicrobial agents provide an advantage for inhibiting or delaying microbial growth on food surfaces, thereby extending shelf life and enhancing food safety (Petchwattana et al., 2021).

Overall, these findings underscore the importance of integrating bioprocess engineering with material characterization. By adjusting the

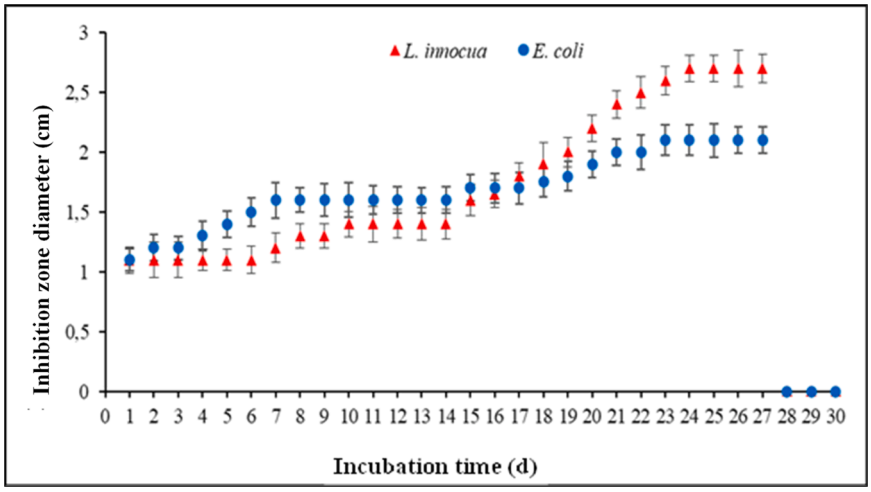

Fig. 5. Kinetics of the antimicrobial activity (inhibition zone diameter) of EPS/geraniol-based film against *E. coli* and L. innocua.

fermentation conditions, it is possible not only to maximize EPS yield but also to tailor the physicochemical properties of the polymer to meet specific performance requirements in active food packaging.

4. Conclusion

This study demonstrates that fed-batch cultivation with continuous feeding of cheese whey, markedly enhanced the EPS production by *H. caseinilytica* K1 compared with batch operation. This strategy also generated higher molecular weight EPS with high content of rhamnose, highlighting the strong influence of bioprocess conditions on polymer structural features. The EPS obtained under continuous feeding (EPS-K1-B3) proved suitable for developing antimicrobial films incorporating geraniol that demonstrated sustained antimicrobial activity during 22 days. Despite the promising results achieved so far, further investigations are needed to characterize the mechanical properties, barrier performance, and microstructure of these antimicrobial films, and also to assess their effectiveness in extending the shelf life of a variety of foods such as fresh fruits and dairy products. Moreover, conducting a life cycle assessment will be essential to evaluate the environmental sustainability of producing antimicrobial films from CW-derived EPS and to determine whether this approach represents an effective sustainable and eco-friendly alternative.

CRediT authorship contribution statement

Samia Azabou: Writing – original draft, Methodology, Investigation, Data curation, Conceptualization. **Ichrak Joulak:** Writing – review & editing, Methodology, Investigation, Data curation. **Patrícia Concórdio-Reis:** Writing – review & editing, Methodology, Investigation. **Cristiana AV Torres:** Writing – review & editing, Methodology, Investigation. **Chantal Sevrin:** Formal analysis. **Christian Grandfils:** Formal analysis. **Hamadi Attia:** Supervision, Resources. **Adem Gharsallaoui:** Writing – review & editing, Supervision, Resources, Conceptualization. **Filomena Freitas:** Writing – review & editing, Supervision, Resources, Conceptualization.

Declaration of competing interest

The authors declare that they have no known competing financial interests or personal relationships that could have appeared to influence the work reported in this paper.

Acknowledgment

This project was financially supported by the Ministry of Higher Education and Scientific Research of Tunisia through the scholarship program “Mobility to Encourage Young Tunisian Researchers” (no. 19PEJC07-02, 2019). Additional funding was provided by FCT – Fundação para a Ciência e a Tecnologia, I.P. (Portugal), through projects UIDP/04378/2020 and UIDB/04378/2020 of the Applied Molecular Biosciences Unit (UCIBIO), as well as project LA/P/0140/2020 of the Associate Laboratory Institute for Health and Bioeconomy (i4HB). The authors also gratefully acknowledge the financial support of Université Claude Bernard Lyon 1, which contributed to the completion of this work during the research stay in France.

Data availability

Data will be made available on request.

References

Antunes, S., Freitas, F., Alves, V. D., Grandfils, C., & Reis, M. A. M. (2015). Conversion of cheese whey into a fucose- and glucuronic acid-rich extracellular polysaccharide by *Enterobacter* A47. *Journal of biotechnology, 210*, 1–7. https://doi.org/10.1016/j.jbiotec.2015.05.013

Bradford, M. M. (1976). A rapid and sensitive method for the quantitation of microgram quantities of protein utilizing the principle of protein-dye binding. *Analytical Biochemistry, 72*, 248–254. https://doi.org/10.1006/abio.1976.9999

Cazon, P., Velazquez, G., Ramírez, J. A., & Vazquez, M. (2017). Polysaccharide-based films and coatings for food packaging: A review. *Food Hydrocolloids, 68*, 136–148. https://doi.org/10.1016/j.foodhyd.2016.09.009

Concordio-Reis, P., Alves, V. D., Moppert, X., Guezennec, J., Freitas, F., & Reis, M. A. M. (2021). Characterization and biotechnological potential of extracellular polysaccharides synthesized by *Alteromonas* strains isolated from French Polynesia marine environments. *Marine Drugs, 19*, 522–537. https://doi.org/10.3390/md19090522

Freitas, F., Alves, V. D., & Reis, M. A. M. (2011). Advances in bacterial exopolysaccharides: From production to biotechnological applications. *Trends in Biotechnology, 29*, 388–398. https://doi.org/10.1016/j.tibtech.2011.03.008

Garcia-Ochoa, F., Santos, V. E., Casas, J. A., & Gómez, E. (2000). Xanthan gum: Production, recovery, and properties. *Biotechnology Advances, 18*, 549–579. https://doi.org/10.1016/S0734-9750(00)00050-1

Gonzalez-Garcia, Y., Heredia, A., Meza-Contreras, J. C., Escalante, F. M. E., Camacho-Ruiz, R. M., & Cordova, J. (2015). Biosynthesis of extracellular polymeric substances by the marine bacterium *saccharophagus degradans* under different nutritional conditions. *International Journal of Polymer Science*, 7–15. https://doi.org/10.1155/2015/526819, 2011.

Haghighi, H., Biard, S., Bigi, F., De Leo, R., Bedin, E., Pfeifer, F., Siesler, F. H., Licciardello, W., & Pulvirenti, A. (2019). Comprehensive characterization of active chitosan-gelatin blend films enriched with different essential oils. *Food Hydrocolloids, 95*, 33–42. https://doi.org/10.1016/j.foodhyd.2019.04.019

Han, M., Xu, J. Z., Liu, Z. M., Qianc, H., & Zhang, W. G. (2018). Co-production of microbial oil and exopolysaccharide by the oleaginous yeast *sporidiobolus pararoseus* grown in fed-batch culture. *RSC Advances, 8*, 3348–3357. https://doi.org/10.1039/C7RA12813D

Hassannia-Kolaee, M., Khodaiyan, F., & Shahabi-Ghahfarrokhi, I. (2016). Modification of functional properties of pullulan–whey protein bionanocomposite films with nanoclay. *Journal of Food Science and Technology, 53*(2), 1294–1302.

Jiang, P., Li, J., Han, F., Duan, G., Lu, X., Gu, Y., & Yu, W. (2011). Antibiofilm activity of an exopolysaccharide from marine bacterium *vibrio sp*. QY10. *PLoS One, 6*, Article 18514. https://doi.org/10.1371/journal.pone.0018514

Joulak, I., Azabou, S., Dumas, E., Freitas, F., Attia, H., & Gharsallaoui, A. (2023). Microencapsulation via spray-drying of geraniol-loaded emulsions stabilized by marine exopolysaccharide for enhanced antimicrobial activity. *Life (Chicago, Ill. : 1978), 13*, 1958. https://doi.org/10.3390/life13101958

Joulak, I., Concórdio-Reis, P., Torres, C. A. V., Sevrin, C., Grandfils, C., Attia, H., Freitas, F., Reis, M. A. M., & Azabou, S. (2022). Sustainable use of agro-industrial wastes as potential feedstocks for exopolysaccharide production by selected *Halomonas* strains. *Environmental Science and Pollution Research, 29*, 22043–22055. https://doi.org/10.1007/s11356-021-17207-w

Joulak, I., Finore, I., Nicolaus, B., Leone, L., Schiano Moriello, A., Attia, H., Poli, A., & Azabou, S. (2019). Evaluation of the production of exopolysaccharides by newly isolated *Halomonas* strains from Tunisian hypersaline environments. *International Journal of Biological Macromolecules, 138*, 658–666. https://doi.org/10.1016/j.ijbiomac.2019.07.128

Le Costaouëc, T., Cérantola, S., Ropartz, D., Ratiskol, J., Sinquin, C., Colliec-Jouault, S., & Boisset, C. (2021). Structural data on a bacterial exopolysaccharide produced by a deep-sea *Alteromonas macleodii* strain. *Carbohydrate Polymers, 90*, 49–59. https://doi.org/10.1016/j.carbpol.2012.04.059

Liu, L., Zhang, X., Yin, L., Zhang, H., Li, J., & Ma, Y. (2025). Advances and challenges in bioproduction of microbial exopolysaccharides: Synthesis mechanisms, engineering strategies, and future perspectives. *Carbohydrate Polymers, 367*, Article 124010. https://doi.org/10.1016/j.carbpol.2025.124010

Liu, L., Du, G., Chen, J., Wang, M., & Sun, J. (2008). Enhanced hyaluronic acid production by a two-stage culture strategy based on the modeling of batch and fed-batch cultivation of *Streptococcus zooepidemicus*. *Bioresource Technology, 99*, 8532–8536. https://doi.org/10.1016/j.biortech.2008.02.035

Lv, P. J., Qiang, S., Liu, L., Hu, C. H., & Meng, Y. H. (2020). Dissolved-oxygen feedback control fermentation for enhancing β-carotene in engineered *Yarrowia lipolytica*. *Scientific Reports, 10*, Article 17114. https://doi.org/10.1038/s41598-020-74074-0

Mabrouki, J., Abbassi, M. A., Khiari, B., Jellali, S., Zorpas, A. A., & Jeguirim, M. (2022). The dairy biorefinery: Integrating treatment process for Tunisian cheese whey valorization. *Chemosphere, 293*, Article 133567. https://doi.org/10.1016/j.chemosphere.2022.133567

Malick, A., Khodaei, N., Benkerroum, N., & Karboune, S. (2017). Production of exopolysaccharides by selected *Bacillus* strains: Optimization of media composition to maximize the yield and structural characterization. *International Journal of Biological Macromolecules, 102*, 539–549. https://doi.org/10.1016/j.ijbiomac.2017.03.151

Öner, E. T., Hernández, L., & Combie, J. (2016). Review of levan polysaccharide: From a century of past experiences to future prospects. *Biotechnology Advances, 34*, 827–844. https://doi.org/10.1016/j.biotechadv.2016.05.002

Ouattara, B., Simard, R. E., Holley, R. A., Piette, G. J., & Bégin, A. (1976). Antibacterial activity of selected fatty acids and essential oils against six meat spoilage organisms. *International Journal of Food Microbiology, 37*, 155–162. https://doi.org/10.1016/s0168-1605(97)00070-6

Petchwattana, N., Naknaen, P., Cha-aim, K., Suksri, C., & Sanetuntikul, J. (2021). Controlled release antimicrobial sachet prepared from poly(butylene succinate)/geraniol and ethylene vinyl alcohol coated paper for bread shelf-life extension application. *International Journal of Biological Macromolecules, 189*, 251–261. https://doi.org/10.1016/j.ijbiomac.2021.08.119

Poli, A., Anzelmo, G., & Nicolaus, B. (2010). Bacterial exopolysaccharides from extreme marine habitats: Production, characterization and biological activities. *Marine Drugs, 8*, 1779–1802. https://doi.org/10.3390/md8061779

Radchenkova, N., Vassilev, S., Martinov, M., Kuncheva, M., Panchev, I., Vlaev, S., & Kambourova, M. (2014). Optimization of the aeration and agitation speed of *Aeribacillus palidus* 418 exopolysaccharide production and the emulsifying properties of the product. *Process Biochemistry (Barking, London, England), 49*, 576–582. https://doi.org/10.1016/j.procbio.2014.01.010

Robert, L., Labat-Robert, J., & Robert, A. M. (2012). Physiology of skin aging. *Clinics in Plastic Surgery, 39*, 1–8. https://doi.org/10.1016/j.cps.2011.09.006

Seviour, R. J., McNeil, B., Fazenda, M. L., & Harvey, L. M. (2011). Operating bioreactors for microbial exopolysaccharide production. *Critical Reviews in Biotechnology, 31*, 170–185. https://doi.org/10.3109/07388551.2010.505909

Shiryanpour, S., Nouri, L., Azizi, M., Najafi, A., & Mohammadi Nafchi, A. (2025). Active chitosan film containing single and double nanoemulsions of *Oliveira decumbens* vent essential oil/anthocyanin of eggplant for chicken preservation. *Journal of Food Measurement and Characterization, 19*, 7381–7403. https://doi.org/10.1007/s11694-025-03477-2

Yang, Y., & Sha, M. (2022). *A beginner's guide to bioprocess modes – Batch, fed-batch, and continuous fermentation (Application note no. 408)*. Eppendorf SE.